Numerical experiments with idealized pore space geometries and shear-thinning fluids

Martin Lanzendörfer

Institute of Hydrogeology,
Engineering Geology and Applied Geophysics

CHARLES UNIVERSITY
Faculty of Science

Disclaimer

Today, Monday came earlier than expected.
Check everything what you read here.
Do not trust anything.
Enjoy.

Part I:
very brief Background

Capillary bundle model & non-Newtonian fluids

Permeability & Pore Size Distribution

- permeability of porous media with respect to shear-thinning fluids *reflects* the pore size distribution (PSD) in the media
- the functional PSD can be (to some extent) recovered from saturated permeability (or infiltration) experiments

Basic concept (better see the references, though)

the capillary bundle model... (with streight capillaries, let us forget the tortuosity for now)

$$v(\dots) = \int_0^1 w(r) \frac{q(r,\dots)}{r^4} \, \mathrm{d}r \approx \sum_{j=1}^{N} w_j \frac{q(r_j,\dots)}{r_j^4}$$

$v(\dots)$ the volumetric flux, ... stand for the hydraulic gradient, fluid, etc.
$q(r,\dots)$ the flow rate through a (cylindrical) capillary of radius r,
r_j, w_j discrete representative capillary radii and the corresponding weights

Capillary bundle model & non-Newtonian fluids

Inverse problems of identifying the discrete representation

- for M flow experiments with the same sample of media one obtains v_i, $i = 1, \dots, M$, and expects

$$v_i = a_{ij}(r_j) w_j , \quad \text{where} \quad a_{ij} = \frac{q_i(r_j)}{r_j^4} .$$

- note that for Newtonian fluid, cylindrical pores $\Longrightarrow$ Hagen–Poisseuille flow, and for the experiments with the pressure gradient J_i (and the viscosity μ_i),

$$q_i(r_j) = \frac{\pi r_j^4}{8\mu_i} J_i \qquad \Longrightarrow \qquad a_{ij}(r_j) = \frac{\pi J_i}{8\mu_i}$$

  so that that matrix $(a_{ij})_{i,j}$ has all columns identical and is thus singular;
- with suitable non-Newtonian fluid(s), the experiments can be designed in such a way, that the columns of $(a_{ij})_{i,j}$ are linearly independent;

Various approaches have appeared (and more may come).

ANA model [1,2,3,4]

- For a shear-thinning power-low fluid, i.e. the fluid with the viscosity

$$\mu = \mu_1 |\mathbf{D}|^{\alpha-1}\,, \quad \text{with } \mu_1 > 0\,,\ 0 < \alpha < 1,$$

one gets (for the head J_i and the rheology $\mu_{1,i}$, α_i in i-th experiment)

$$q_i(r_j) = C_i J_i^{(1/\alpha_i)} r_j^{3+(1/\alpha_i)} \qquad \Longrightarrow \qquad a_{ij}(r_j) = C_i J_i^{(1/\alpha_i)} r_j^{(1/\alpha_i)-1}$$

so that linearly independent columns can be achieved by having distinct α_i, which is done by using different concentrations of xanthan in water;

- For more realistic descriptions, such as e.g. Cross model

$$\mu = \mu_\infty + \frac{\mu_0 - \mu_\infty}{1 + G|\mathbf{D}|^{-\alpha}}\,, \quad \text{with } \mu_0, \mu_\infty, G > 0\,,\ 0 < \alpha < 1,,$$

one can still use some semi-analytic solutions...
One can use experiments with different fluids and/or pressure gradients (see in what follows).

---

[1] Abou Najm M.R., Atallah N.M. (2016). *Vadose Zone J.* 15, 1–5.
[2] Atallah N.M., Abou Najm M.R. (2019). *Eur. J. Soil Sci.* 70, 257–267.
[3] Basset C.N., Abou Najm M.R., Ammar A., et al. (2019). *Vadose Zone J.*, 18(1), 1–13.
[4] Hauswirth S.C., Abou Najm M.R., Miller C.T. (2019). *Water Resour. Res.* 55(8), 7182–7195.

Various approaches have appeared (and more may come).

ANA model [1,2,3,4] : Inverse problems—types

- Type 1: For given radii r_j, compute the weights w_j.
  Leads to linear problem (with constraints, however).
  - In the original works: $M = N$ so that the matrix is square.
    There are some more subtleties. . . , MATLAB `lsqlin` is called to get w_j.
  - In this presentation's examples, $N \leq M$.
    Here only $w_j \geq 0$ is required, MATLAB `lsqnonneg` is called.
- Type 2: For given weights w_j, compute the radii r_j.
  Nonlinear (and even more interesting).
  - Not commented here . . . work in progress.
- Type 3: a combination.

---

[1] Abou Najm M.R., Atallah N.M. (2016). *Vadose Zone J.* 15, 1–5.
[2] Atallah N.M., Abou Najm M.R. (2019). *Eur. J. Soil Sci.* 70, 257–267.
[3] Basset C.N., Abou Najm M.R., Ammar A., et al. (2019). *Vadose Zone J.*, 18(1), 1–13.
[4] Hauswirth S.C., Abou Najm M.R., Miller C.T. (2019). *Water Resour. Res.* 55(8), 7182–7195.

Various approaches have appeared (and more may come).

Yield Stress fluids Method[5,6]

- The yield stress (& shear-thinning) fluid model (although for the same fluid in practice!) is utilized;
- given the particular yield stress fluid and hydraulic gradient, the flow only occurs in pores larger than of certain threshold radius;
- the algorithm used is thus different . . . although the concept is the same.

[5] Rodríguez de Castro A., et al. (2019). *Transport in Porous Media* 130(3), 799–818.
[6] Rodríguez de Castro A., et al. (2020). *Comp. Chem. Eng.* 133.

Part II:
Examples of open problems

Not addressed here, only pinpointed.
Many issues are related to the mathematical description, not to the data.

Open problems

. . . Anyone can invent *problems*. They are mentioned here only to point out that many of them can be addressed with the help of artificial data. . .

- The power-law fluid and the yield stress fluid are two extremal models, each in it's own way. How do the corresponding algorithms cope with realistic fluids?
- Given the particular fluid and some expectation about PSD, can one suggest an optimal set of flow experiments (pressure drops, polymer concentrations)?
- That being said, can we define what would the optimality mean at the first place?
- Given the experimental data and the resulting PSD signature, can we assess the uncertainty?

- How are certain types of non-trivial PSDs (multiple porosity materials) represented?
- How are other idealized pore space models represented in the capillary bundle framework?
- Is there any use of the framework for the solute transport properties?

- The solutions for ANA problem types 1 and 2 that are unique for $N = M$ for the power-law fluid, may not be in general unique for realistic fluids with Newtonian regimes.
- What are the numerical aspects of the inversion problem?
- Can the influence of the numerical error / uncertainty be estimated? (If so, one could optimize the experiments in order to reduce it.)

Part III:
Artifitial data—Numerical experiments

Simple examples: non-cylidrical capillary tubes.

Unidirectional flow in a tube

Steady generalized Stokes flow

$$\operatorname{div} \mathbf{T} = \mathbf{0}\,, \quad \text{where} \quad \begin{aligned} \mathbf{T} &= -p\mathbf{I} + 2\mu(|\mathbf{D}|)\mathbf{D}, \\ \mathbf{D} &= \tfrac{1}{2}\left(\nabla \mathbf{v} + \nabla \mathbf{v}^T\right) \end{aligned}$$

Simple unidirectional flow in a capillary tube

$$\left.\begin{aligned} \mathbf{v}(\mathbf{x}) &= (0, 0, u(x_1, x_2)), \\ \nabla p(\mathbf{x}) &= (0, 0, J)\,, \quad J \in \mathbb{R} \end{aligned}\right\} \implies \begin{aligned} \operatorname{div}\left(\mu(|\nabla u|)\nabla u\right) = -J \quad \text{in } \Omega \subset \mathbb{R}^2 \\ \Omega = \text{cross section of the tube} \end{aligned}$$

This is a very simple scalar elliptic PDE. Numerical solutions were computed by finite element method implemented in FEniCS.[7]

[7] Logg A., et al. (2012). Automated Solution of Differential Equations by the Finite Element Method. Springer.

Unidirectional flow in a tube: Example 1

Inter-cylindrical pore

Instead of cylindrical tube, we consider the (free) space in between (solid) cylindres:

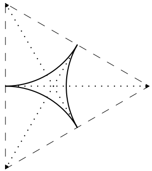

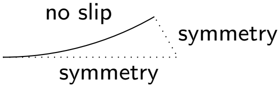

Due to the sharp corners, it is not clear (well, it was not to me) how it will be represented by cylindrical "functional pores".

Example of flow

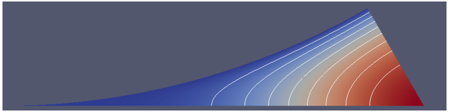

velocity u

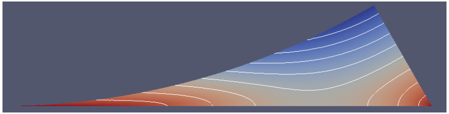

viscosity $\mu(|\nabla u|)$

Unidirectional flow in a tube: Example 1

Examples of weights computed from simulated permeability experiments

On the plot at the next page:

- the radius of the simulated pore (defined by the circle of equivalent area) indicated by circle;
- for N given radii r_j (in $10^{-5} - 4 \times 10^{-4}$), the weights $w(r_j)$ are identified based on M experiments, with $M \geq N$;
- experiments are simulated numerically: the same fluid (Cross model), M hydraulic gradients;
- for reduced number of given pore radii, $N < M$, either all experiments are used or different subsets of experiments are selected and compared;

Identification of weights

See Problem-type 1[8,9,10] simplified: no porosity, no strictly positive weights, no tortuosity. Find $w_j \geq 0$ (using MATLAB nonnegative linear least squares `lsqnonneg` solver) such that:

$$A_{ij} w_j = b_i, \quad \text{where} \begin{cases} A_{ij} = q_i(r_j)/r_j^4, & q_i(r_j) \text{ flow rate though a cylindrical pore} \\ b_i = q_i, & q_i \text{ data from the simulated experiment} \end{cases}$$

[8] Abou Najm M.R., Atallah N.M. (2016). *Vadose Zone J.* 15, 1–5.
[9] Atallah N.M., Abou Najm M.R. (2019). *Eur. J. Soil Sci.* 70, 257–267.
[10] Hauswirth S.C., Abou Najm M.R., Miller C.T. (2019). *Water Resour. Res.* 55(8), 7182–7195.

Unidirectional flow in a tube: Example 1

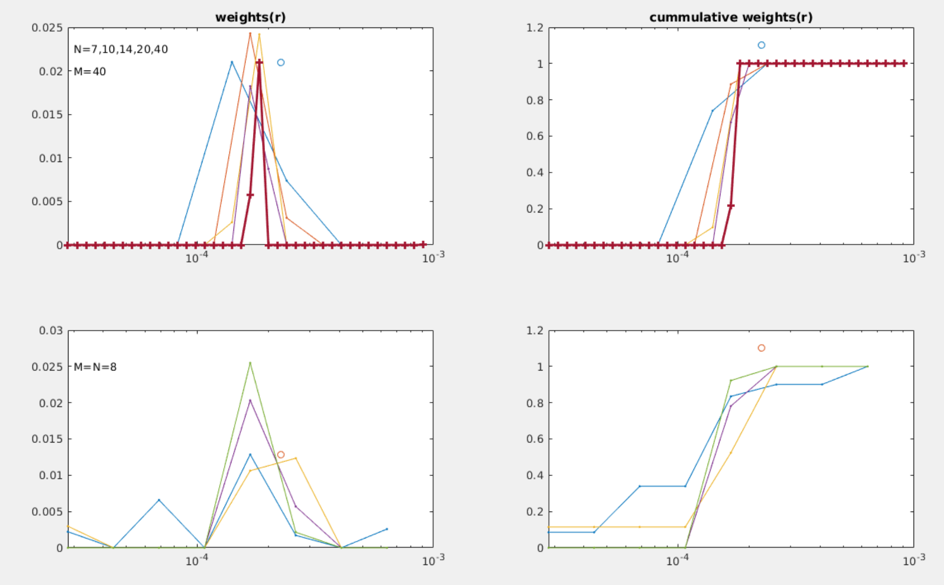

Unidirectional flow in a tube: Example 1

Commentary

- According to the first row, it works nicely. The functional PSD signature computed for 40 radii using 40 permeability experiments (purple with crosses) captures one representative radius of our inter-cylindrical pore. The reduced signatures computed for sparser grids of radii, but computed from the same full data set, approximate nicely that solution.
- The second row shows the results for $N = 8$ pore radii, computed using different subsets of $M = 8$ experimental data points. Note the false positive weights for small pore radii.
- However, the appearance of these false small pores is obviously caused by the following insufficiency of the (yellow and light blue) data sets: due to small hydraulic gradients and the Cross model, the rheology was almost Newtonian within the simulated capillary.

Unidirectional flow in a tube: Example 2

Deformed inter-cylindrical pore

Toy example: the previous cross section geometry deformed ($3\times$ elongated along one axis and $3\times$ shortened along the other; so it is more like a fissure). The goal is produce wider range of effective pore sizes.

Examples of weights computed from simulated permeability experiments

On the plot at the next page:

- similarly as before;
- only results with $N = M$ are shown, based on 32 simulated experiments;
- for $N < 32$ (second and third row), different subsets of experiments are compared;

Unidirectional flow in a tube: Example 2

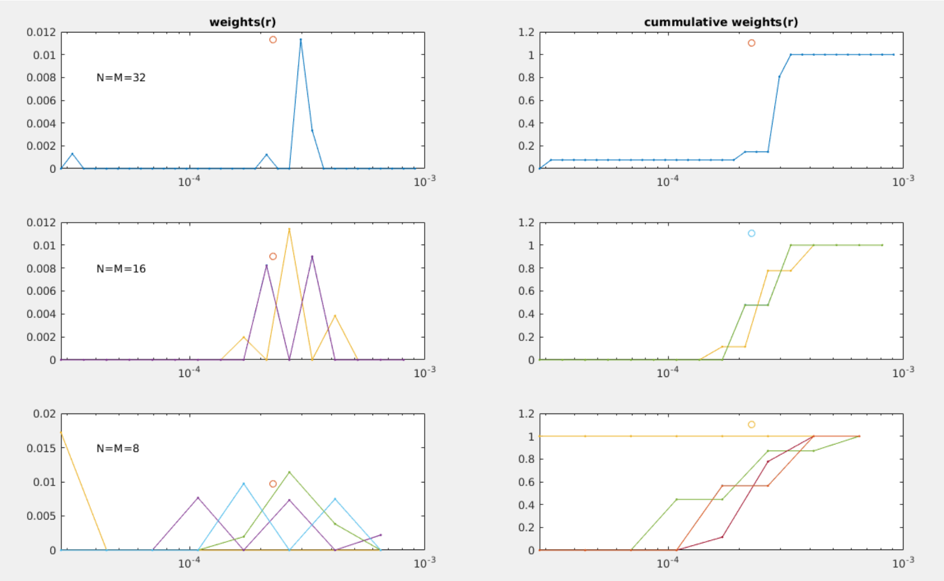

Unidirectional flow in a tube: Example 2

Commentary

- Note the smallest pore at the first row. It seems as it *attempts* to represent the thinnest part of the geometry. It's position is usually among the smallest radii of the given range, and the value of the weight appears to depend on the given range of radii as well.
- In contrast, the singular (yellow) weight at the third row reveals something else. It corresponds to the selection of the 8 data points (experiments) with the lowest hydraulic gradient, i.e. for the smallest velocities and shear rates. Same as in the previous example, the viscosity given by Cross model is practically Newtonian in this regime.
- The two plots at the second row correspond to 16 given radii and two different subsets of 16 experiments. However, the purple plot (green on the right) is also equivalent to the result from *all* 32 *data points* (by the least squares method).
- The same holds true for the third row and the light blue (red on the right) plot: exactly the same 8 weights would be computed from all 32 experiments.

Thank you for your attention!

If you happened to print this. . .
. . . it is still green, more or less.

CHARLES UNIVERSITY
Faculty of Science